Journal of the Iranian Chemical Society
https://doi.org/10.1007/s13738-019-01727-x

ORIGINAL PAPER

Ni-guanidine@MCM-41 NPs: a new catalyst for the synthesis of 4,4′-(arylmethylene)-bis-(3-methyl-1-phenyl-1*H*-pyrazol-5-ols) and symmetric di-aryl sulfides

Hossein Filian[1,2] · Arash Ghorbani-Choghamarani[3] · Elham Tahanpesar[2]

Received: 15 December 2018 / Accepted: 28 June 2019

Abstract
In this work, the surface of mesoporous MCM-41 was modified with guanidine, and then, Nickel particles have become immobilized on its surface (Ni-guanidine@MCM-41NPs). This heterogeneous catalyst has been identified by various techniques including: low-angle X-ray diffraction, scanning electron microscopy, energy-dispersive X-ray spectroscopy, inductively coupled plasma, thermal gravimetric analysis and N_2 adsorption–desorption measurement isotherms, and its catalytic application was studied in the synthesis of 4,4′-(arylmethylene)-bis-(3-methyl-1-phenyl-1*H*-pyrazol-5-ol) derivatives and symmetric di-aryl sulfides. The prepared organometallic complex could be isolated, post-reaction, by simple filtration for several consecutive cycles without a notable change in its catalytic activity.

Keywords Mesoporous MCM-41 · Nickel · Guanidine · Sulfides

Introduction

Multicomponent reactions are becoming a strategic tool for the synthesis of biological heterocyclic compounds [1–4]. The major advantages of multicomponent reactions are high atom economy, time saving and one-pot synthesis without isolation of generating by-products or intermediates [2–7]. Among the various N-heterocyclic compounds, the bis-pyrazolones and pyrazolones were paid much attention for their different biological applications, such as antibacterial [8], antifilarial agents [9], antitumor [10], cytokine inhibitors [11], selective COX-2 inhibitory [12], pesticides [13], fungicides [14], anti-inflammatory [15] and dyes [16]. Moreover, these compounds were used as extracting agents for some metal ions in analytical chemistry [17, 18] and ligands in coordination chemistry [17–19].

✉ Arash Ghorbani-Choghamarani
a.ghorbani@ilam.ac.ir; arashghch58@yahoo.com

1 Department of Chemistry, Khuzestan Science and Research Branch, Islamic Azad University, Ahvaz, Iran

2 Department of Chemistry, Ahvaz Branch, Islamic Azad University, Ahvaz, Iran

3 Department of Chemistry, Faculty of Science, Ilam University, P.O. Box 69315516, Ilam, Iran

Besides, it is worth mentioning that Carbon–heteroatom bond formation is the most fundamental reactions in modern organic synthesis. In this respect, such reactions can be regarded as powerful tools for the production of several important pharmaceutical and biological compounds [20–22]. Among them, C–S coupling reaction has a great demand in organic chemistry and pharmacological sciences [21–24], i.e., sulfide derivatives which are used as potent drugs for HIV, Alzheimer, cancer and Parkinson diseases [25, 26]. In addition, sulfide derivatives are used as starting materials for the preparation of sulfoxides and sulfones [22]. However, C–S coupling and multicomponent reactions will proceed in the presence of a catalyst in order to achieve a tolerable selectivity and isolated yields.

Nanoparticles as catalysts or support for catalysts have become a significant field of organic methodology researches [27, 28]. The potential advantages of nanoparticles in catalysis applications can be named as simplified recovery, reusability and efficiency activity due to high surface area [28, 29]. Therefore, nanoparticles could lead to novel and environment-friendly catalytic applications for industry and academic researches [30]. In this sense, mesoporous materials such as MCM-41 have been widely used in catalysis fields [31], drug delivery systems [32], adsorption [33, 34], extraction [35] and energy [36]. MCM-41 has unique properties such as high stability (more than 900 °C), simple preparation

Published online: 08 July 2019

and separation and large specific surface area (> 1000 m^2/g), which leads to ease of its functionalization [37–40]. These unique properties of mesoporous MCM-41 will make it a wonderful support for various catalysts [41, 42]. Therefore, herein, a new complex of nickel on mesoporous MCM-41 was reported as a high efficient catalyst in organic reactions.

Experimental

Preparation of guanidine complex of nickel supported on the surface of MCM-41 (Ni-guanidine@MCM-41NPs)

Initially, mesoporous MCM-41 modified by 3-chloropropyltrimethoxysilane (nPrCl-MCM-41NPs) was synthesized according to our previous reported method [29]. For immobilization of the guanidine on the surface of nPrCl-MCM-41NPs, guanidine nitrate (2 mmol) and Na_2CO_3 (2 mmol) were added to mixture of nPrCl-MCM-41NPs (1 g) in toluene (10 ml), and the reaction mixture stirred for 24 h at 100 °C. The obtained guanidine@MCM-41NPs was filtered and washed with ethanol for several times and, then, dried under air atmosphere. In the final step, immobilization of nickel onto guanidine@MCM-41NPs was performed by mixing the guanidine@MCM-41NPs (1 g) and $Ni(NO_3)_2{\cdot}6H_2O$ (2 mmol) in ethanol. The resulted mixture was stirred for 20 h under reflux conditions. The obtained Ni-guanidine@MCM-41NPs was filtered and washed with ethanol for several times and, then, dried under air atmosphere (Scheme 1).

General procedure for the synthesis of 4,4′-(arylmethylene)-bis-(3-methyl-1-phenyl-1*H*-pyrazol-5-ols) derivatives

A mixture of 3-methyl-1-phenyl-5-pyrazolone (2 mmol), aldehyde (1 mmol) and Ni-guanidine@MCM-41NPs nanocatalyst (0.05 g) in acetonitrile was stirred at 80 °C, and the progress of the reaction was monitored by TLC. Upon the completion of the reaction, the mixture was cooled down to room temperature and the catalyst was separated by simple filtration and washed with hot ethanol. Then, the solvent was evaporated and, consequently, pure 4,4′-(arylmethylene)-bis-(3-methyl-1-phenyl-1*H*-pyrazol-5-ol) derivatives were obtained in high yields (Scheme 2).

General procedure for the synthesis of symmetric di-aryl sulfides

A mixture of Ni-guanidine@MCM-41NPs (0.05 g), aryl halide (1 mmol), sulfur (0.5 mmol) and potassium hydroxide (0.5 g) was stirred at 110 °C in DMSO (3 ml). Upon the completion of the reaction, the mixture was cooled down to room

Scheme 1 Synthesis of Ni-guanidine@MCM-41NPs

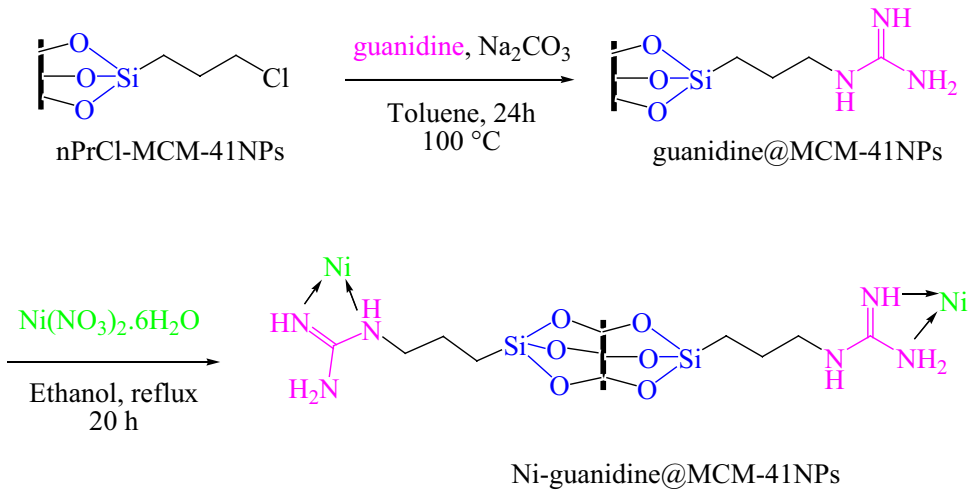

Scheme 2 Ni-guanidine@MCM-41NPs catalyzed the synthesis of 4,4′-(arylmethylene)-bis-(3-methyl-1-phenyl-1*H*-pyrazol-5-ol) derivatives

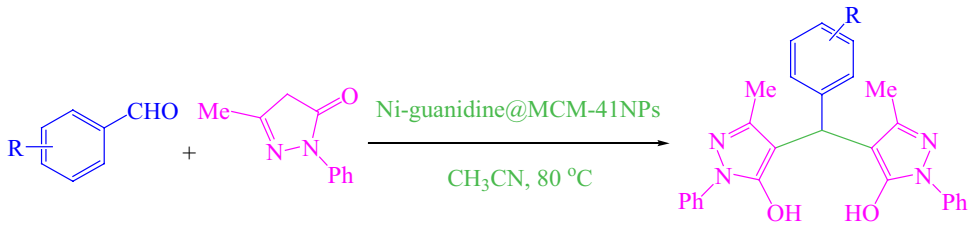

temperature and the catalyst was separated by simple filtration, and then, the filtrated solution was extracted with ethyl acetate. In addition, the organic layer was dried with anhydrous Na_2SO_4, and organic solvent was evaporated to afford pure products (Scheme 3).

Selected spectral data

di-p-Tolylsulfane (Table 5, Entry 5): ^{1}H NMR (500 MHz, DMSO-d6): δ_H 2.26 (s, 6H), 7.17–7.18 (d, J = 7 Hz, 4H), 7.37–7.39 (d, J = 7 Hz, 4H) ppm; ^{13}C NMR (125 MHz, DMSO-d6) δ 21.0, 128.6, 130.5, 131.2, 133.1 ppm.

4,4′-((2-Bromophenyl)methylene)bis(3-methyl-1-phenyl-1*H*-pyrazol-5-ol) (Table 3, Entry 3): ^{1}H NMR (500 MHz, DMSO-d6): δ_H 2.32 (s, 6H), 5.14 (s, 1H), 7.12–7.15 (t, J = 10 Hz, 1H), 7.22–7.25 (t, J = 5 Hz, 2H), 7.33–7.36 (t, J = 5 Hz, 1H), 7.42–7.45 (t, J = 10 Hz, 4H), 7.56–7.58 (d, J = 10 Hz, 1H), 7.72–7.73 (d, J = 5 Hz, 4H), 7.86–7.88 (d, J = 5 Hz, 1H), 11.68 (br, 1H), 13.82 (br, 1H) ppm; ^{13}C NMR (125 MHz, DMSO-d6) δ 12.6, 34.8, 104.5, 121.0, 123.3, 126.1, 127.9, 128.8, 129.4, 131.0, 133.3, 137.6, 141.5, 146.5 ppm.

4,4′-((3,4-Dimethoxyphenyl)methylene)bis(3-methyl-1-phenyl-1*H*-pyrazol-5-ol) (Table 3, Entry 7): ^{1}H NMR (500 MHz, DMSO-d6): δ_H 2.34 (s, 6H), 3.68 (s, 3H), 3.71 (s, 3H), 4.91 (s, 1H), 6.84–6.88 (t, J = 10 Hz, 2H), 6.93 (s, 1H), 7.22–7.25 (t, J = 10 Hz, 2H), 7.43–7.46 (t, J = 10 Hz, 4H), 7.73–7.75 (d, J = 10 Hz, 4H), 11.81 (br, 1H), 14.11 (br, 1H) ppm; ^{13}C NMR (125 MHz, DMSO-d6) δ 12.1, 33.4, 56.0, 105.4, 112.1, 112.2, 119.8, 121.0, 126.0, 129.4, 135.5, 137.9, 146.7, 147.7, 148.9 ppm.

4,4′,4′′,4′′′-(1,4-Phenylenebis(methanetriyl))tetrakis(3-methyl-1-phenyl-1*H*-pyrazol-5-ol) (Table 3, Entry 10): ^{1}H NMR (500 MHz, DMSO-d6): δ_H 2.28 (s, 12H), 4.87 (s, 2H), 7.17–7.68 (m, 24H), 12.43 (br, 2H), 14.10 (br, 2H) ppm; ^{13}C NMR (500 MHz, DMSO-d6) δ 12.1, 33.3, 121.1, 126.0, 127.4, 129.3, 140.5, 146.7 ppm.

Result and discussion

The synthesized nanocatalyst (Ni-guanidine@MCM-41NPs) has been characterized by the XRD, SEM, EDS, ICP, TGA and N_2 adsorption–desorption measurement isotherms techniques.

Catalyst characterizations

The XRD pattern of Ni-guanidine@MCM-41NPs which is shown in Fig. 1 consists of an intense peak at 2θ = 2.58 which is allocated to the (100) of mesoporous channels regularity of MCM-41 after immobilization of organic layers and nickel complex onto MCM-41 channels [30]. However, upon post-synthetic grafting, the (110) and (200) reflections became weaker and, also, the intensity of d100 decreased. This is due to the irregular immobilization of Ni complex onto channels of MCM-41 [30].

The morphological features of MCM-41 and Ni-guanidine@MCM-41NPs were investigated by SEM technique. The SEM images of MCM-41 and Ni-guanidine@MCM-41NPs are shown in Fig. 2. As illustrated in (Fig. 2a), particles of mesoporous MCM-41 were observed between 60–90 nm with homogeneous size and spherical morphology.

As it is evident from the SEM image of Ni-guanidine@MCM-41NPs, the diameter of the prepared nanoparticles is about 60–90 nm with homogeneous size and spherical morphology (Fig. 2b) which is in agreement with SEM images of MCM-41. Therefore, size and shape of the catalyst have not been changed after the grafting process.

In order to determine the elemental composition of Ni-guanidine@MCM-41NPs nanocatalyst, the components of catalyst were analyzed using EDS (Fig. 3). As depicted, the EDS spectrum of Ni-guanidine@MCM-41NPs all of the elements: Si, O, C, N and nickel species was observed in the catalyst composition. Moreover, the exact amount of nickel in catalyst which was obtained by ICP technique was found to be 1.6×10^{-3} mol g^{-1}.

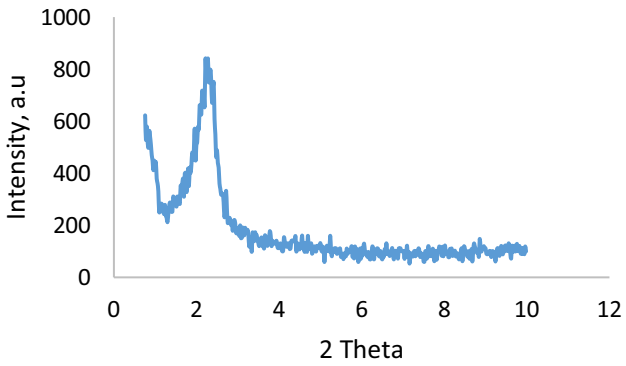

Fig. 1 Low-angle XRD patterns of Ni-guanidine@MCM-41NPs

Scheme 3 Ni-guanidine@MCM-41NPs catalyzed the synthesis of symmetric di-aryl sulfides

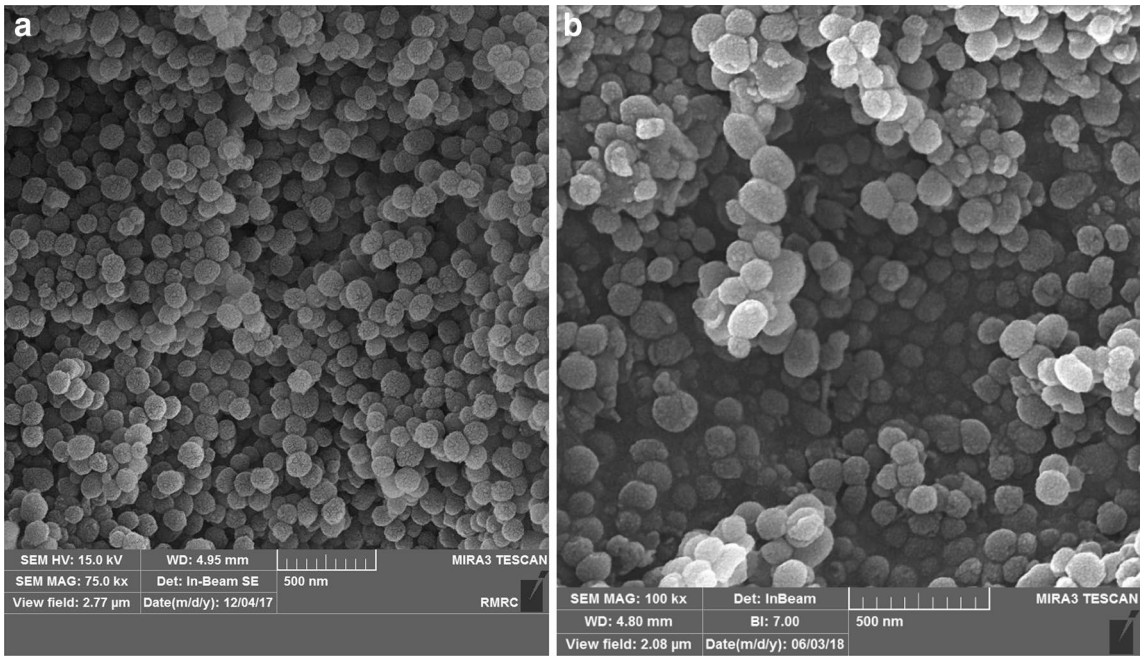

Fig. 2 SEM images of **a** MCM-41 and **b** Ni-guanidine@MCM-41NPs

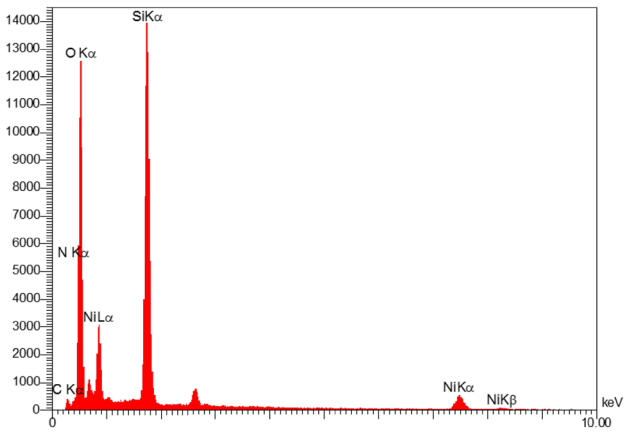

Fig. 3 EDS image of Ni-guanidine@MCM-41NPs Nano-material

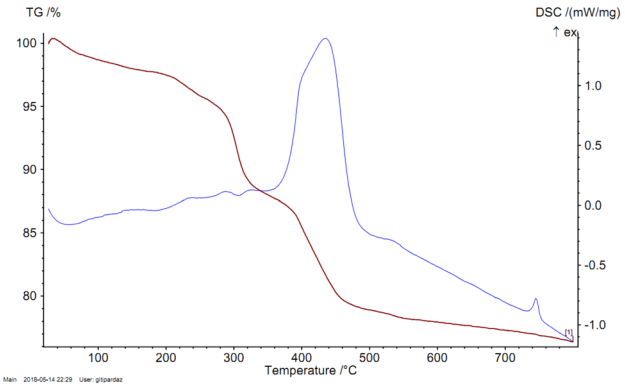

Fig. 4 TGA analysis of Ni-guanidine@MCM-41NPs

The immobilization of guanidine-Ni organometallic complex on the surface of MCM-41NPs was also studied by TGA analysis. The TGA diagram of the Ni-guanidine@MCM-41NPs is shown in Fig. 4 which illustrates a three-step weight loss while increasing the temperature. The first step shows a small mass loss (which is about 2%) at below 100 °C may be due to the removal of the physically and chemically absorbed solvents or surface hydroxyl groups [29, 30]. The second and third steps between 100–460 °C and 460–800 °C with 17 and 4% of weight loss are attributed to the decomposition of organic layers [4] and decomposition of the silanol groups, respectively [29] (Fig. 4).

The N_2 adsorption and desorption isotherms of Ni-guanidine@MCM-41NPs are illustrated in Fig. 5, and the results are summarized in Table 1. This diagram displays isotherm of type IV according to the IUPAC, which can be regarded as the mesoporous structure of Ni-guanidine@MCM-41NPs [43]. Based on Brunauer–Emmett–Teller (BET), the surface area for Ni-guanidine@MCM-41NPs is 428 m^2/g, which is lower than the surface area of mesoporous MCM-41 (1372 m^2/g) [30]. The average pore diameter and pore volume of Ni-guanidine@MCM-41NPs are 1.29 nm and 0.61 $cm^3\ g^{-1}$, respectively, which are lower than MCM-41 (2.45 nm and 1.51 $cm^3\ g^{-1}$) [29, 30]. The decrease in surface area, average pore diameter and pore volume of Ni-guanidine@MCM-41NPs is due to

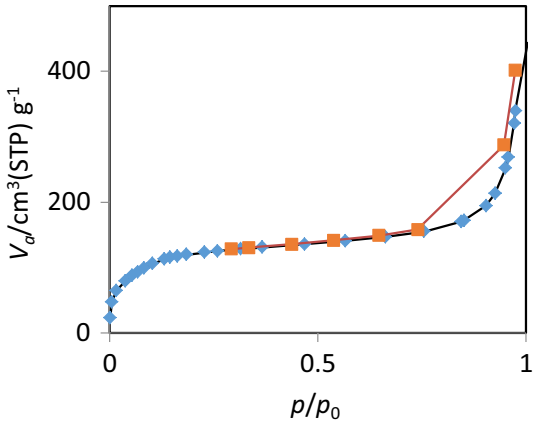

Fig. 5 N_2 adsorption–desorption isotherms of Ni-guanidine@MCM-41NPs

Table 1 Texture properties of Ni-guanidine@MCM-41NPs

Sample name	SBET ($m^2\ g^{-1}$)	DBJH (nm)	V Total ($cm^3\ g^{-1}$)
Ni-guanidine@MCM-41NPs	428	1.29	0.61

the immobilization of organic layers and nickel complex onto MCM-41.

Study of catalytic property

Catalytic activity of Ni-guanidine@MCM-41NPs was investigated in the synthesis of 4,4′-(arylmethylene)-bis-(3-methyl-1*H*-pyrazol-5-ol) (Scheme 2) and symmetric di-aryl sulfides (Scheme 3).

Initially, the reaction conditions for the synthesis of 4,4′-(arylmethylene)-bis-(3-methyl-1*H*-pyrazol-5-ol) have been optimized for different reaction parameters including the amount of catalyst, nature of solvent and temperature (Table 2). At first, the condensation of benzaldehyde and 3-methyl-1-phenyl-5-pyrazolone for the synthesis of 4,4′-(arylmethylene)-bis-(3-methyl-1*H*-pyrazol-5-ol) has been selected as model reaction.

At the outset, the effect of different amounts of Ni-guanidine@MCM-41NPs catalyst in the model reaction was examined (Table 2, entries 1–4) and different solvents (Table 2, entries 4–8). The best results were obtained in acetonitrile as solvent using 0.05 g of Ni-guanidine@MCM-41NPs. Also, the effect of temperature was studied (Table 2, entries 8–10). Accordingly, the best result was obtained at 80 °C (Table 2, entry 3).

In order to explore the generality and scope of this method, various aldehydes (contenting electron-donating and electron-withdrawing functional groups) were tested under optimized reaction conditions (Table 3). As shown in Table 3, all products were obtained in high yields. Also, terephthaldehyde was converted to the corresponding product in 75% of yield (Table 3, entry 10).

Table 2 Screening of the reaction parameters for the synthesis of 4,4′-(arylmethylene)-bis-(3-methyl-1-phenyl-1*H*-pyrazol-5-ol)

Entry	Catalyst (mg)	Solvent	Temperature (°C)	Time (min)	Yield (%)[a]
1	20	Acetonitrile	80	30	73
2	40	Acetonitrile	80	30	85
3	50	Acetonitrile	80	30	92
4	60	Acetonitrile	80	30	92
5	50	Ethyl acetate	80	60	85
6	50	Ethanol	80	60	80
7	50	Acetone	80	60	64
8	50	Solvent-free	120	20	5
9	50	Acetonitrile	25	30	10
10	50	Acetonitrile	70	30	75

[a]Isolated yield

In the second part of our study, the catalytic ability of Ni-guanidine@MCM-41NPs for the synthesis of symmetric di-aryl sulfides from C–S coupling reaction was considered under various reaction conditions (Scheme 3). For this purpose, the coupling of iodobenzene with S_8 was selected as the model reaction. In this sense, the model reaction was examined in various solvents (Table 4, entries 6–9) and in the presence of different amounts of Ni-guanidine@MCM-41NPs (Table 4, entries 1–6). The reaction did not proceed in the absence of the catalyst (Table 4, entry 1). As shown in Table 4, increase in the amount of the Ni-guanidine@MCM-41NPs led to an increase in the isolated products, whose best results were obtained with 0.05 g of Ni-guanidine@MCM-41NPs in dimethyl sulfoxide (Table 4, entry 5). Then, the model reaction was examined in various bases (Table 4, entries 9–12) at different temperatures (Table 4, entries 12–17). Among the various bases, the highest yield has been obtained using KOH at 110 °C (Table 4, entry 5).

After optimization of the reaction conditions, the catalytic activity of Ni-guanidine@MCM-41NPs was extended to a wide range of aryl halides including aryl iodides, aryl bromides and aryl chlorides.

The results of this study are summarized in Table 5. As shown, a wide range of aryl halides bearing electron-donating and electron-withdrawing functional groups was successfully coupled with S_8 and all products were obtained in excellent yields.

Table 3 Preparation of 4,4′-(arylmethylene)-bis-(3-methyl-1-phenyl-1*H*-pyrazol-5-ols) derivatives catalyzed by Ni-guanidine@MCM-41NPs

Entry	Product	Time (min)	Yield (%)	M.P. (°C)	M.P. (°C) [Lit.]
1	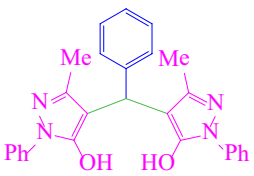	30	92	168–170	170–172 [19]
2	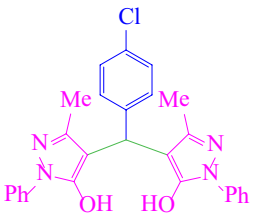	25	90	210–215	213–215 [10]
3	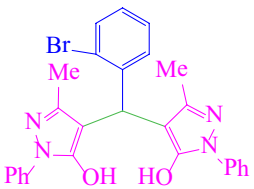	20	90	195–200	198–200 [18]
4	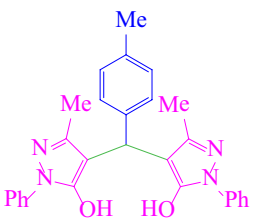	35	90	202–203	202–204 [19]
5	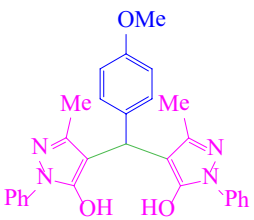	40	83	170–175	173–175 [10]
6	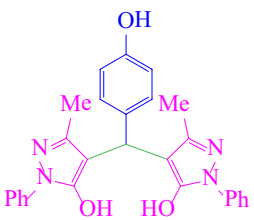	35	80	150–155	153–155 [10]
7	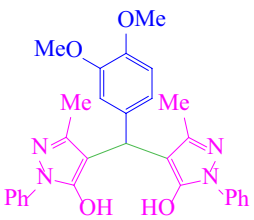	60	87	194–196	194–196 [10]

Table 3 (continued)

Entry	Product	Time (min)	Yield (%)	M.P. (°C)	M.P. (°C) [Lit.]
8	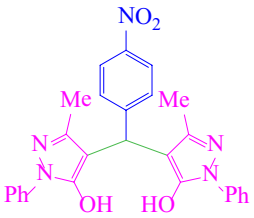	15	85	220–228	225–227 [18]
9	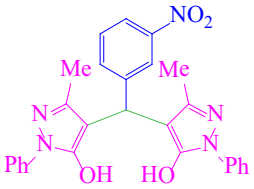	20	83	145–150	151–153 [11]
10	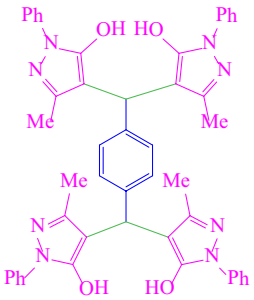	75	75	210–215	214–216 [18]

Table 4 Screening of the reaction parameters for the synthesis of symmetric di-aryl sulfides in 150 min

Entry	Catalyst (g)	Solvent	Base	Temperature (°C)	Yield (%)[a]
1	–	DMSO	KOH	110	–[b]
2	0.02	DMSO	KOH	110	35
3	0.03	DMSO	KOH	110	57
4	0.04	DMSO	KOH	110	75
5	0.05	DMSO	KOH	110	94
6	0.06	DMSO	KOH	110	94
7	0.05	Water	KOH	110	–[b]
8	0.05	PEG	KOH	110	–[b]
9	0.05	DMF	KOH	110	65
10	0.05	DMSO	Na_2CO_3	110	30
11	0.05	DMSO	K_2CO_3	110	40
12	0.05	DMSO	NaOH	110	73
13	0.05	DMSO	KOH	25	–[b]
14	0.05	DMSO	KOH	40	25
15	0.05	DMSO	KOH	60	47
16	0.05	DMSO	KOH	80	65
17	0.05	DMSO	KOH	120	94

[a]Isolated yield

[b]No reaction

Catalyst reusability

The reusability of Ni-guanidine@MCM-41NPs was examined in the model reaction. After completion of the reaction, the catalyst was recovered by centrifugation and, then, reused again for 6 more runs without loss of its catalytic activity (Fig. 6), signifying that the nickel leaching from Ni-guanidine@MCM-41NPs is very low.

Conclusion

In conclusion, we have successfully immobilized the nickel complex of guanidine onto pores of MCM-41. Then, this nanocatalyst was characterized by various techniques such as: XRD, SEM, EDS, ICP, TGA and BET. The catalyst shows high catalytic activity in 4,4′-(arylmethylene)-bis-(3-methyl-1-phenyl-1*H*-pyrazol-5-ol) and C–S coupling reaction toward preparation of symmetric di-aryl sulfides. The remarkable advantages of this procedure include simple work-up procedure, operational simplicity, high efficiency of catalyst which led to high yields of the products in short reaction times and its environmentally friendly nature. Also,

Table 5 C–S coupling of aryl halides with S_8 catalyzed by Ni-guanidine@MCM-41NPs

Entry	Aryl halide	Product	Time (h)	Yield (%)[a]	M.P. (°C)	M.P. (°C) [Lit.]
1	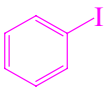	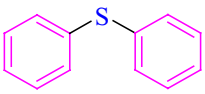	2.5	94	Oil	Oil [44]
2	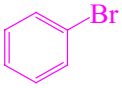	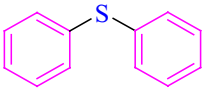	6	85	Oil	Oil [44]
3	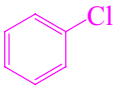	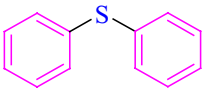	17	63	Oil	Oil [44]
4	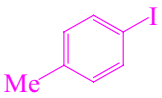	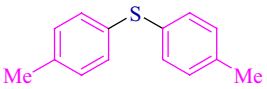	12	80	Oil	Oil [44]
5	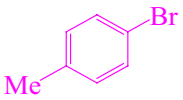	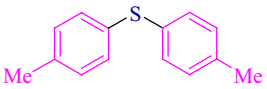	14	70	Oil	Oil [44]
6	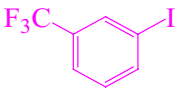	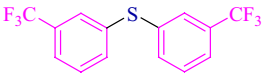	6	83	Oil	Oil [44]
7	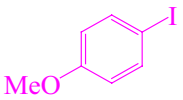	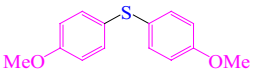	5	87	Oil	Oil [44]
8	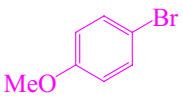	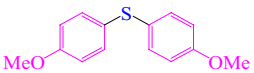	6.5	80	Oil	Oil [44]
9	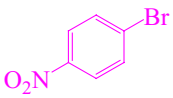	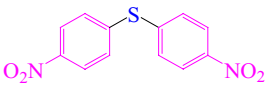	2	60	150–158	157–159 [44]
10	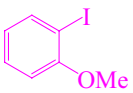	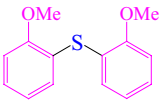	9	85	Oil	Oil [44]

[a]Isolated yield

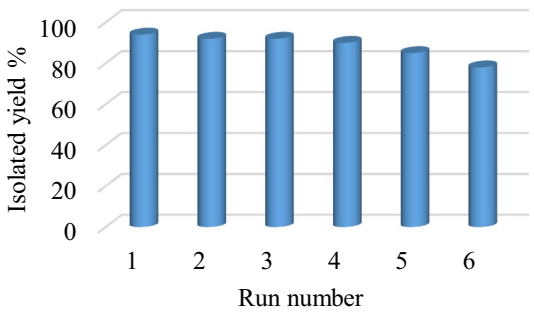

Fig. 6 Recycling experiment of Ni-guanidine@MCM-41NPs in synthesis of symmetric di-aryl sulfides from coupling of iodobenzene with S_8

this catalyst can be recovered by simple filtration and reused for several times without loss of performance.

Acknowledgements This work was supported by the research facilities of Ahvaz Branch, Islamic Azad University, Ahvaz, Iran.

References

1. C.M. Marson, Chem. Soc. Rev. **41**, 7712 (2012)
2. B. Jiang, T. Rajale, W. Wever, S.J. Tu, G. Li, Chem. Asian J. **5**, 2318 (2010)
3. A. Dömling, W. Wang, K. Wang, Chem. Rev. **112**, 3083 (2012)
4. A. Ghorbani-Choghamarani, M. Mohammadi, T. Tamoradi, M. Ghadermazi, Polyhedron **158**, 25 (2019)

5. H. Wu, Y. Gou, J. Wang, L. Tao, Macromol. Rapid Commun. **39**, 1800064 (2018)
6. D. Das, ChemistrySelect **1**, 1959 (2016)
7. C. Shen, X.F. Wu, Chem. Eur. J. **23**, 2973 (2017)
8. R.N. Mahajan, F.H. Havaldar, P.S. Fernandes, J. Indian Chem. Soc. **68**, 245 (1991)
9. P.M.S. Chauhan, S. Singh, R.K. Chatterjee, ChemInform **24**, 72 (1993)
10. M. Keshavarz, M. Vafaei-Nezhad, Catal. Lett. **146**, 353 (2016)
11. M. Baghernejad, K. Niknam, Int. J. Chem. **4**, 52 (2012)
12. C.S. Yao, C.X. Yu, S.J. Tu, D.Q. Shi, X.S. Wang, Y.Q. Zhu, H.Z. Yang, J. Fluor. Chem. **128**, 105 (2007)
13. A.R. Moosavi-Zare, M.A. Zolfigol, M. Zarei, A. Zare, V. Khakyzadeh, A. Hasaninejad, Appl. Catal. A Gen. **467**, 61 (2013)
14. M.N. Elinson, A.S. Dorofeev, R.F. Nasybullin, G.I. Nikishin, Synthesis (Stuttg) **2008**, 1933 (2008)
15. K. Niknam, D. Saberi, M. Sadegheyan, A. Deris, Tetrahedron Lett. **51**, 692 (2010)
16. E. Soleimani, S. Ghorbani, M. Taran, A. Sarvary, Comptes Rendus Chim. **15**, 955 (2012)
17. A. Hasaninejad, M. Shekouhy, A. Zare, S.M.S.H. Ghattali, N. Golzar, J. Iran. Chem. Soc. **8**, 411 (2011)
18. K. Niknam, M.S. Habibabad, A. Deris, N. Aeinjamshid, Chem. Mon. **144**, 987 (2013)
19. K. Niknam, S. Mirzaee, Synth. Commun. **41**, 2403 (2011)
20. Y. Zhang, K.C. Ngeow, J.Y. Ying, Org. Lett. **9**, 3495 (2007)
21. I.P. Beletskaya, V.P. Ananikov, Chem. Rev. **111**, 1596 (2011)
22. L. Chen, A. Noory Fajer, Z. Yessimbekov, M. Kazemi, M. Mohammadi, J. Sulfur Chem. **40**, 451 (2019)
23. L. Rout, T.K. Sen, T. Punniyamurthy, Angew. Chem. Int. Ed. **46**, 5583 (2007)
24. M. Moorthy, A. Govindaraj, B. Madheswaran, B. Kannan, R. Rangappan, ChemistrySelect **1**, 4833 (2016)
25. D. Giuliani, A. Ottani, D. Zaffe, M. Galantucci, F. Strinati, R. Lodi, S. Guarini, Neurobiol. Learn. Mem. **104**, 82 (2013)
26. L. Argueta-Figueroa, O. Martínez-Alvarez, J. Santos-Cruz, R. Garcia-Contreras, L.S. Acosta-Torres, J. de la Fuente-Hernández, M.C. Arenas-Arrocena, Mater. Sci. Eng. C **76**, 1305 (2017)
27. V. Polshettiwar, R.S. Varma, Green Chem. **12**, 743 (2010)
28. A. Ghorbani-Choghamarani, M. Mohammadi, Z. Taherinia, J. Iran. Chem. Soc. **16**, 411 (2019)
29. M. Nikoorazm, A. Ghorbani-Choghamaranai, M. Khanmoradi, P. Moradi, J. Porous Mater. **25**, 1831 (2018)
30. H. Filian, A. Ghorbani-Choghamarani, E. Tahanpesar, J. Porous Mater. (2018) **(in press)**
31. N. Gutta, V.K. Velisoju, A. Chatla, V. Boosa, J. Tardio, J. Patel, V. Akula, Energy Fuels **32**, 4008 (2018)
32. G. Maria, A.I. Stoica, I. Luta, D. Stirbet, G.L. Radu, Microporous Mesoporous Mater. **162**, 80 (2012)
33. A. Benhamou, J.P. Basly, M. Baudu, Z. Derriche, R. Hamacha, J. Colloid Interface Sci. **404**, 135 (2013)
34. A.G. Thomé, F. Schroeter, P. Bottke, J. Wittayakun, F. Roessner, Microporous Mesoporous Mater. **274**, 342 (2019)
35. S.A. Idris, S.R. Harvey, L.T. Gibson, J. Hazard. Mater. **193**, 171 (2011)
36. Y. Sun, X.W. Liu, W. Su, Y. Zhou, L. Zhou, Appl. Surf. Sci. **253**, 5650 (2007)
37. M. Abdollahi-Alibeik, M. Pouriayevali, Catal. Commun. **22**, 13 (2012)
38. X. Wang, G. Wu, J. Li, N. Zhao, W. Wei, Y. Sun, J. Mol. Catal. A: Chem. **276**, 86 (2007)
39. Y. Huang, W. Hao, G. Ding, M.Z. Cai, J. Organomet. Chem. **715**, 141 (2012)
40. B. Karami, M. Farahi, S. Akrami, D. Elhamifar, New J. Chem. **42**, 12811 (2018)
41. M. Eslami, M.G. Dekamin, L. Motlagh, A. Maleki, Green Chem. Lett. Rev. **11**, 36 (2018)
42. J.N. Appaturi, M. Selvaraj, S.B. Abdul Hamid, M.R. Bin Johan, Microporous Mesoporous Mater. **260**, 260 (2018)
43. T. Tamoradi, M. Ghadermazi, A. Ghorbani-Choghamarani, Catal. Lett. **148**, 857 (2018)
44. A. Ghorbani-Choghamarani, Z. Seydyosefi, B. Tahmasbi, Appl. Organomet. Chem. **32**, e4396 (2018)